Geothermometry and kinetics in a two-spinel peridotite nodule, Colorado Plateau

Douglas Smith

Department of Geological Sciences
University of Texas, Austin, Texas 78712

and Michael F. Roden

Department of Earth and Planetary Sciences
Massachusetts Institute of Technology, Cambridge, Massachusetts 02139

Abstract

Compositions and zoning of minerals in a two-spinel peridotite from minette in the Navajo volcanic field on the Colorado Plateau provide unusual opportunities to compare geothermometers at low mantle temperature and to study equilibration rates. The xenolith contains pleonaste ($Mg_{.55}Fe_{.45}Al_{1.62}Fe_{.10}Cr_{.28}O_4$) and magnetite ($Mg_{.16}Fe_{.89}Mn_{.01}Al_{.18}Fe_{1.38}Cr_{.32}Ti_{.06}O_4$) related by granule exsolution, together with olivine (Fo_{85}), orthopyroxene (3.5% Al_2O_3), and clinopyroxene. Both two-spinel equilibria and several olivine-pleonaste geothermometers indicate equilibration near or below 700°C, confirming the general accuracy and continued equilibration of these geothermometers at low temperatures. Calculated olivine-magnetite temperatures are much too high. Two-pyroxene temperatures are near 800°C.

Olivine is zoned in Ca, Fe, and Mg within 50 μm of spinel by exchange with local grain boundary melts. Gradients at pleonaste-magnetite contacts were caused by multicomponent diffusion after heating by minette; effects include slight "uphill" diffusion of Cr. Effective binary diffusion coefficients near 1100°C, estimated by comparison with gradients in olivine, are near 10^{-11} cm²/sec for Al in magnetite and 10^{-12} cm²/sec for Al in pleonaste; an average Mg value is in the same range.

The time interval between plucking of the inclusion and minette solidification is calculated as about 60 hours, consistent with ascent times calculated assuming Newtonian viscosity for the minette magmas. The temperatures calculated for olivine–spinel equilibria confirm the low temperatures in the upper mantle of the Colorado Plateau inferred from hydrated lherzolites in nearby diatremes of serpentinized ultramafic microbreccia.

Introduction

Interpretation of temperatures estimated for mineral equilibration in peridotite is often complicated by disagreement between temperatures calculated by different methods (*e.g.,* Finnerty and Boyd, 1979). The disagreements arise not only because of inconsistent calibrations of geothermometers but also because the compositions of minerals adjust at different rates to changes in pressure and temperature. For instance, Smith and Levy (1976), Roeder *et al.* (1979), and Fabries (1979) have suggested that spinel–olivine pairs continue to equilibrate with cooling to temperatures below those recorded by two-pyroxene geothermometers. The lherzolite inclusion described here contains olivine, orthopyroxene, clinopyroxene, and two spinels. The two-spinel assemblage offers unusual opportunities to compare spinel-silicate equilibria at low temperatures and to examine the effects and rates of multicomponent diffusion in spinels. The assemblage also helps to characterize the thermal history of the upper mantle below the Colorado Plateau.

The two-spinel inclusion was collected in a talus block of minette at the foot of a thick lava flow capping Zilditloi Mountain in the Navajo volcanic field in westernmost New Mexico (109°00'W, 35°54'N). The minette is a potassic, mafic lava with phenocrysts of clinopyroxene and phlogopite and altered

phenocrysts of olivine in a groundmass rich in sanidine. The host is unanalyzed but very similar to nearby minette with olivine described by Allen and Balk (1954) and Roden and Smith (1979). The minette of Zilditloi Mountain also contains many inclusions of feldspathic rocks and pyroxenite. The locality lies within 8 km of two large pipes of serpentinized ultramafic microbreccia, Buell Park and Green Knobs, which have abundant peridotite inclusions (Smith and Levy, 1976; Roden and Smith, 1979).

Description of peridotite

Petrography and mineralogy

The inclusion is angular, equant, and about 15 mm in maximum dimension. The mode (980 points) is 62% olivine, 17% orthopyroxene, 16% clinopyroxene, 5% spinel, and a trace of phlogopite. The texture is equant-granuloblastic, as defined by Harte (1976); most grain diameters are in the range 0.5–1.5 mm. Olivine grains appear unstrained. Most pyroxene grains optically appear free from exsolution lamellae; some contain very thin lamellae of pyroxene, however, and the cores of some grains are packed with very small, oriented blades and rods of spinel (?).

The discrete spinel grains are opaque in thin sections of normal thickness. In reflected light, most grains are clearly composite, one part being a whiter, magnetite-rich phase and the other a grayer, pleonaste-rich one. The boundaries between the two phases are generally simple and smooth (Fig. 1). The two parts apparently formed by granule exsolution from a single spinel. The color changes are gradational over a few micrometers distance rather than abrupt. The proportions of the two phases appear about equal; in point-counting, 25 of the 46 points on spinel were on pleonaste.

Effects of late-stage interaction with the host minette are imprinted upon the peridotite in several ways. Curving fracture planes dotted with spheres and tubules cut silicates and grain boundaries; the inclusions (glass?) are typically several micrometers in size. Locally at the margin of the inclusion and within it are small volumes of pryoxenes and olivine with rare, identifiable feldspar with grain sizes of a few micrometers to a few tens of micrometers: these volumes are common at spinel–pyroxene contacts, though many such contacts are apparently unaffected (Fig. 1). The fine-grained volumes, which comprise about 4% of the inclusion, probably crystallized from or in contact with grain-boundary melts formed by heating by the host magma and the accompanying decompression. Since these volumes are best-developed near and at the margins of the inclusion, the minette magma may also have contributed constituents to some of these melts.

Mineral chemistry

Mineral analyses (Table 1) were made using the ARL–EMX electron probe with three crystal spectrometers at the University of Texas. A few analyses were checked with the automated MAC–5–SA3 probe at the California Institute of Technology; agreement was good, and data for Na, Cr, and Ti for analysis 4 (Table 1) are from this instrument. Data corrections were based upon the method of Bence and Albee (1968) and the factors of Albee and Ray (1970). Eight grains of olivine, three grains of each pyroxene, and five composite spinel grains were investigated. Pyroxenes were analyzed both by moving core regions under a broad beam (20 μm diameter) during analysis and by using a focussed beam (1–3 μm diameter) at single points near pyroxene rims. Differences between cores and rims are not systematic, but they do record minor but real inhomogeneity, as expected from the visible lamellae in some pyroxene cores. Interiors of olivine grains are homogeneous. Interiors of spinel grains are homogeneous except in a few anomalous areas, perhaps near hidden contacts. Zoning at contacts is discussed in a later section.

The silicate chemistry is not typical of mantle lherzolite, as the olivine and orthopyroxene are relatively iron-rich; the mg-values (about 0.85) of these phases fall at the iron-rich limit of typical Group I nodules, as defined by Frey and Prinz (1978). Their Group II nodules are more iron-rich and typically have pyroxenes richer in alumina and poorer in chrome than those in the rock studied here. Other atypical lherzolite nodules with similar mineral compositions have been described, however, by Frey and Prinz (1978) and by White (1966). In contrast, all lherzolite nodules described from the nearby Green Knobs and Buell Park diatremes have typical Group I silicate chemistry (Smith and Levy, 1976).

One of the spinels is a chromian pleonaste, the other a chromian magnetite. Pleonaste is common but magnetite is rare in peridotite nodules. If compositions of the two spinels (Table 1) are combined in equal proportions to approximate the parent spinel before exsolution, the resulting composition is much richer in ferric iron than typical spinels in lherzolite nodules (Haggerty, 1976). Similar pairs of spinels,
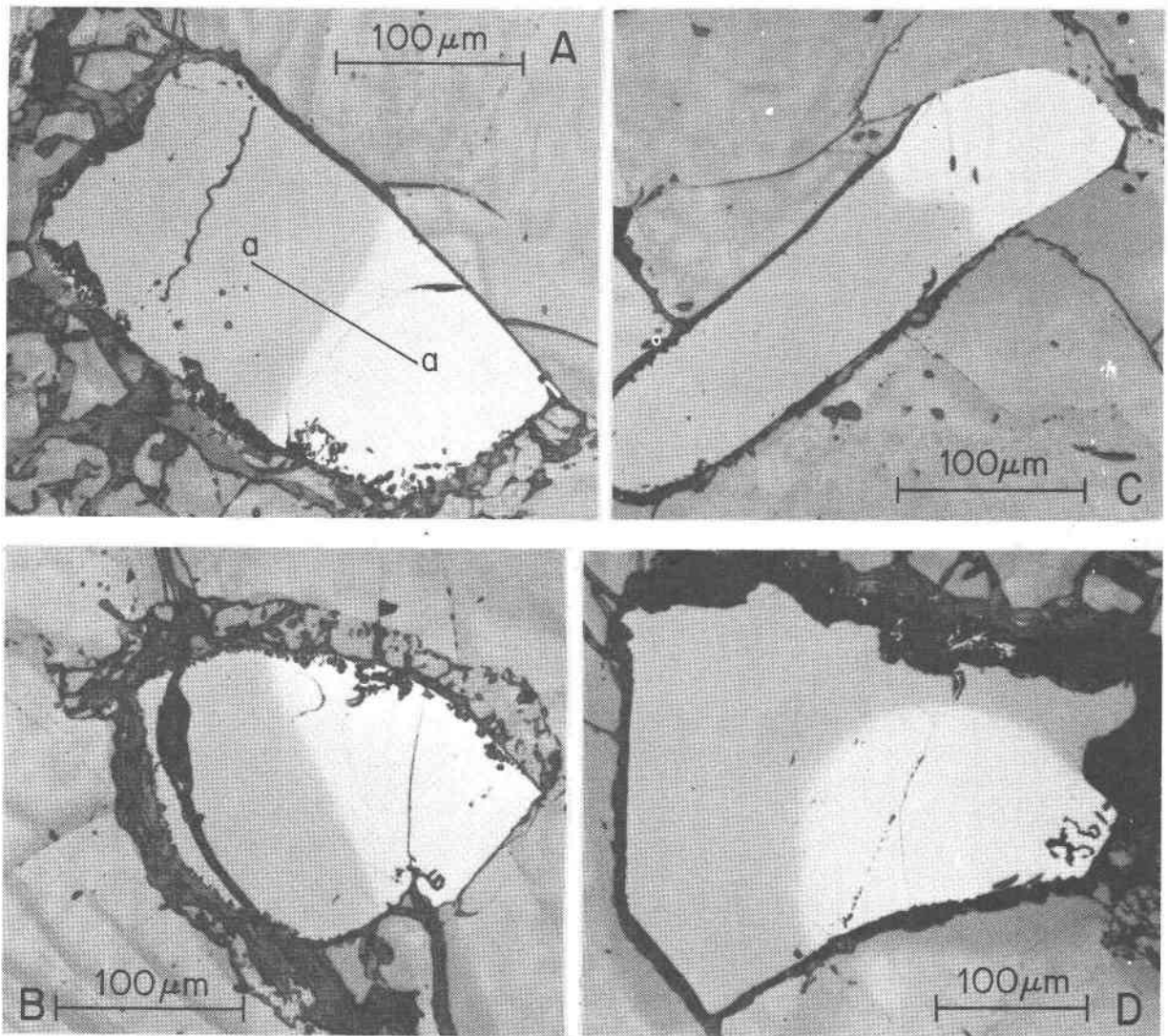
Fig. 1. Photomicrographs of composite spinel grains (reflected light). The traverse data shown in Figs. 4 and 5 were taken along the line a–a in (A). Scale bars are 100 micrometers. Note the recrystallized zones in the lower left of (A) and at the upper spinel contact of (B); the zones are interpreted as the products of local melts at grain boundaries.

first analyzed by Muir and Naldrett (1973), have been described from peridotite emplaced in the crust.

Petrology

The peridotite nodule has had a complex temperature history, here subdivided into these stages: (I) cooling within the mantle from high temperatures, with adjustments of mineral textures and chemistry, including granule exsolution of magnetite and pleonaste from a single spinel; (II) heating as the small inclusion was incorporated in the minette magma; (III) maintenance at high temperature during transportation to the surface and crystallization of the

magma, with formation of local grain-boundary melts, especially near spinel-pyroxene contacts; (IV) cooling within the crystallized minette lava flow at the surface. Stage I may have occupied over a billion years, as the minette was erupted about 25 m.y. ago (Roden et al., 1978) and the last major igneous activity on the Colorado Plateau was the formation of diabase and basalt about 1100 m.y. ago (Silver, 1963). The minette source was deeper than about 130 km (Ehrenberg, 1979), and the thermal event which generated the minette may not have affected the much shallower spinel peridotite. The general homogeneity of the spinel interiors is evidence that they

Table 1. Representative electron probe analyses

	1	2	3	4	5	6	7	8	9
SiO_2	54.8	55.2	51.3	51.7	40.1				
TiO_2	0.19	0.14	0.62	0.61		0.07	0.13	2.25	2.76
Al_2O_3	3.65	3.38	5.13	4.60		49.6	50.1	3.95	4.85
Cr_2O_3	0.22	0.20	0.44	0.38	0.02	12.6	12.2	11.2	10.5
* Fe_2O_3						5.67	5.20	50.9	49.6
* FeO	9.95	9.64	4.85	4.71	14.5	19.5	18.2	29.2	28.8
MnO	0.27	0.27	0.13	0.16	0.26	0.20	0.12	0.32	0.28
MgO	31.0	30.9	14.9	14.9	45.2	13.4	14.2	3.07	3.70
CaO	0.53	0.47	22.1	22.5					
Na_2O			1.12	1.08					
	100.7	100.2	100.6	100.6	100.2	101.0	100.2	100.9	100.4

1. Orthopyroxene (A9), broad central area. 2. Orthopyroxene (A8), point at rim. 3. Clinopyroxene (A11), broad central area. 4. Clinopyroxene (A18), point at rim. 5. Olivine (A6). 6. Pleonaste (A2), same composite as A4. 7. Pleonaste (AA1), same composite as AA5. 8. Magnetite (A4), same composite as A2. 9. Magnetite (AA5), same composite as AA1.

* In silicates all Fe is reported as FeO. In spinels, Fe_2O_3 and FeO are calculated assuming stoichiometry.

were unaffected by stages II–IV, and hence all grain interiors apparently approached equilibration during a long period of relatively constant temperature (Stage I). In contrast, compositions of intergrown spinels in rocks exposed at the surface of the earth may have continued to adjust to slowly decreasing temperatures during uplift (e.g., Steele et al., 1977). The two-spinel pairs in the inclusion thus provide an unusual opportunity to compare geothermometers.

Geothermometry

Temperatures (Table 2) were calculated for olivine-spinel pairs using three proposed geothermometers (Fujii, 1978; Roeder et al., 1979; Fabries, 1979). Compositions were also compared with the graphical summaries of Evans and Frost (1975) prepared for natural spinels equilibrated at about 700°C. The postitions of the pleonaste-olivine data on the Evans–Frost plot suggest equilibration below 700°C; this temperature estimate is probably more reliable than any other which can be made with present data, since the Evans–Frost spinels at the same YCr (Cr/(Cr + Al + Fe³⁺)) are similar in composition to the pleonastes studied here, though slightly more magnesian.

For the pleonaste-olivine pairs, no choice can be made between the results of the algorithms of Fujii (1978) and Fabries (1979). Roeder et al. (1979) state that their algorithm may give too high temperatures at low YCr, as also suggested by the results in Table 2. None of the three geothermometers works well for magnetite–olivine pairs, and small variations in composition lead to extreme temperature differences: as pointed out by Roeder et al. (1979), the distribution of Mg and Fe²⁺ between magnetite-rich spinel and olivine is unlikely to be useful as a geothermometer.

Experimental data for calibration of a 2-spinel geothermometer are available only on the Mg- and Cr-free hercynite-magnetite join, which has an asymmetric miscibility gap with a critical temperature near 860°C (Turnock and Eugster, 1962). The effects of Cr are qualitatively outlined by the studies of natural spinels by Evans and Frost (1975) and Steele et al. (1977): the miscibility gap between pleonaste and magnetite-rich spinels steadily diminishes with increasing Cr until it vanishes at a YCr of about 0.45 at 700°C. Less is known about the effects of Mg–Fe²⁺ substitution; Berg (1976) suggests that the miscibility gap for magnesian pleonaste and magnetite is much

Table 2. Comparative geothermometry

Two-pyroxene temperatures (1)

Pairs of central areas: 779, 786, 841°C

Pair of rim points: 797°C

Spinel-olivine (Fo85) temperatures

	(2)	(3)	(4)
Pleonaste	737	541	636°C
Pleonaste	797	607	679°C
Magnetite	924	2229	1275°C
Magnetite	1033	3468	1467°C

(1) Wells, 1977; (2) Roeder et al. 1979; (3) Fujii, 1978; (4) Fabries, 1979.

wider than for pure Fe–Al–O spinels at 765°C. Two spinel pairs from the inclusion are compared with those selected from other natural occurrences in Figure 2. Comparison with the compositions reported by Berg (1976), Springer (1974), and Steele *et al.* (1977) suggests equilibration below 800°C, likely near or below 700°C, but a more definite statement cannot be made on the basis of the available data. Nonetheless, the two-spinel occurrence clearly supports the general validity of low temperatures calculated for olivine-aluminous spinel pairs by the methods of Table 2.

Two-pyroxene temperatures (Table 2) calculated by the method of Wells (1977) are near 800°C, distinctly higher than the temperatures below 700°C thought most reasonable for olivine–spinel equilibration. The two-pyroxene temperatures are very sensitive to the calculated Mg–Fe occupancy in the clinopyroxene M2 position at Fe-poor compositions and low temperatures, because of the slope and location of the clinopyroxene solvus. Experimental calibration is all at higher temperatures, and selection of appropriate thermodynamic models at these lower temperatures is difficult. The temperature difference may be due to these difficulties, or it may be due to slower pyroxene equilibration rates. Existing geothermometers based upon Al_2O_3 in orthopyroxene have not been applied, since they are appropriate only when coexisting spinels are predominately the $MgAl_2O_4$ end member (Danckwerth and Newton, 1978). When orthopyroxene geothermometers are better developed, the data from this inclusion should be useful for additional comparative geothermometry. The following core (C) and rim (R) weight percents of CaO and Al_2O_3, respectively, document the degree of internal equilibration of the orthopyroxene: C, 0.53, 3.65; C, 0.56, 3.36; C, 0.43, 3.44; R, 0.47, 3.38; R, 0.52, 3.40: R, 0.38, 3.35.

In summary, the mineral data indicate that cooling during Stage I continued to near 700°C at a rate sufficiently slow to homogenize olivine and to eliminate pronounced gradients in the exsolving spinels. Minor inhomogeneities are still present in pyroxene, and the extent to which the pyroxenes approached equilib-
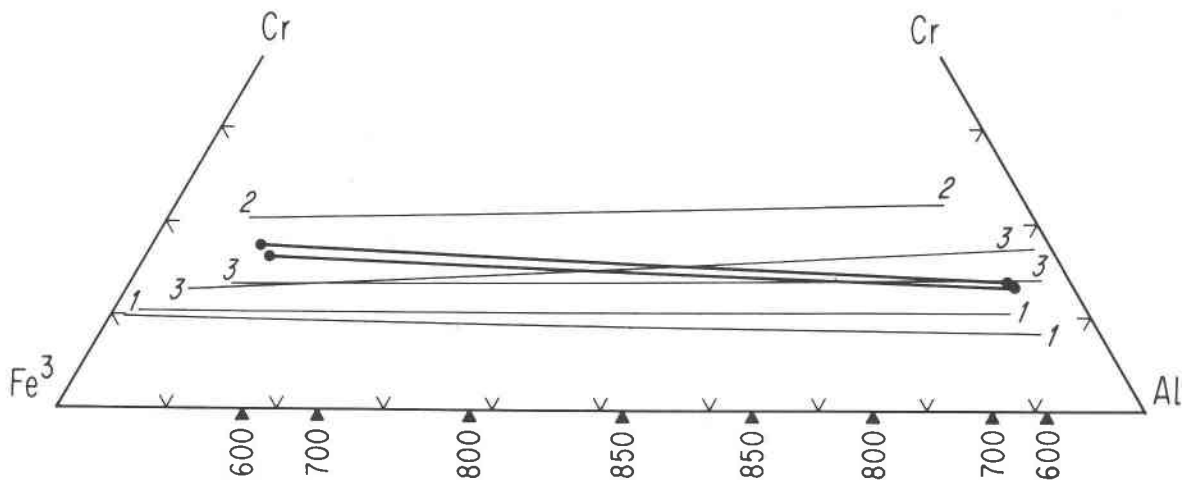

Fig. 2. Compositions of two pairs of intergrown spinels, shown together with selected pairs from Springer (1974)—(1), Muir and Naldrett (1973)—(2), and Steele *et al.* (1977)—(3). Numbers at the base of the diagram are temperatures (°C) for the Cr-free, Mg-free magnetite-hercynite solvi as determined by Turnock and Eugster (1962).

rium at these low temperatures is unclear. Similar low temperatures were inferred for final equilibration of spinel–olivine pairs in lherzolite inclusions at the nearby Green Knobs diatreme by Smith and Levy (1976), so they presumably characterized this region of the upper mantle about 25 m.y. ago.

Compositional zoning

Gradients at olivine grain boundaries

Ca, Fe, and Mg were measured at 3 μm intervals across two olivine-pleonaste and two olivine-magnetite contacts. Olivine crystals are zoned within about 50 μm of these grain boundaries (Fig. 3). Interiors of olivine grains are homogeneous (near 14.3 wt.% FeO, 0.01 CaO), but margins are more iron-rich, more calcic, and less magnesian (16–23 wt.% FeO, 0.10 CaO). Olivine is more iron-rich adjacent to magnetite than to pleonaste (20–23% compared to 16–17%). The consistency of analytical sums calculated for olivine assuming stoichiometry and the antithetic behavior of Fe and Mg indicate that secondary fluorescence did

not make an important contribution to the observed profiles. No zoning was detected in either olivine or orthopyroxene at a mutual contact.

In contrast to olivine, spinel grains are not systematically zoned at spinel–olivine contacts. No zoning was detected in either of the two magnetite grains at these contacts (Fig. 3B). One pleonaste grain appeared unzoned, while within 20 μm of the olivine contact the other is slightly enriched in both magnesium and total iron (and hence probably depleted in ferrous iron and aluminum or chromium).

The increase in Ca as well as in Fe in olivine at contacts with spinel, and the lack of systematic zoning in spinel at these contacts, require that at least one additional phase participated in the exchange with olivine. This phase was likely the grain-boundary melt inferred from recrystallization at some grain boundaries (Figs. 1A, 1B). For instance, though olivine–spinel contacts appear unaltered for the crystal traversed for Figure 3A, a finely recrystallized zone 5–20 μm wide occurs at pleonaste–orthopyroxene and magnetite–orthopyroxene contacts of the same composite spinel grain. The observation that the ex-
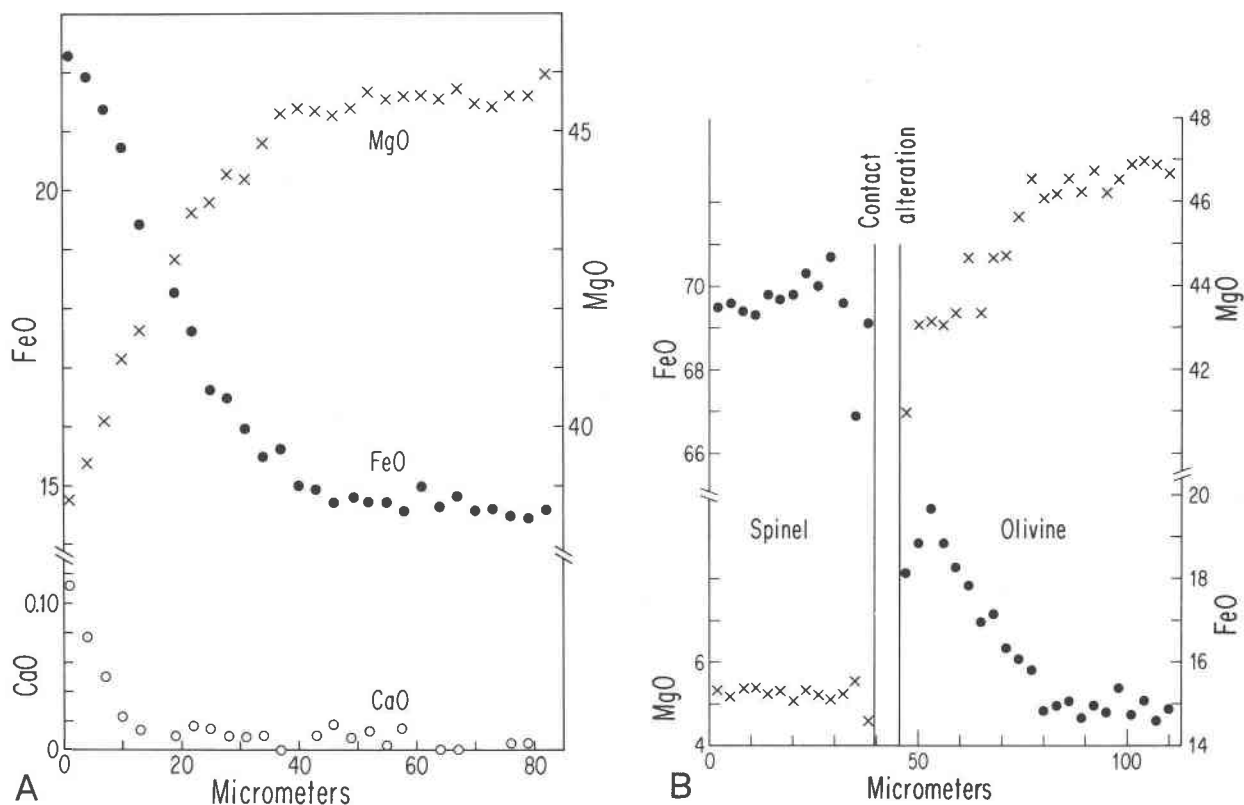

Fig. 3. (A) Weight percents of FeO, MgO, and CaO in olivine measured at 3 μm intervals away from a contact with magnetite. (B) Weight percents of FeO and MgO measured at 3 μm intervals across a contact between another olivine-magnetite pair. The high MgO content of the spinel is anomalous. Two points (not shown) in the contact zone were on another phase, perhaps an alteration product.

tent of iron enrichment in olivine depends upon whether the olivine is in contact with magnetite or with pleonaste is evidence that the melt composition depended upon the contacting phases. Presumably such disequilibrium melts were closer to equilibrium with spinel than with olivine. After they crystallized, cooling (Stage IV) must have been sufficiently rapid to forestall creation of observable diffusion gradients within the spinel due to exchange with olivine.

The assumption that the diffusion profiles within olivine were created during Stage III and were little modified by subsequent cooling during Stage IV is consistent with the observations discussed above. With additional assumptions for the average magma temperature and the Fe–Mg interdiffusion coefficient in the olivine, the approximate duration of Stage III can be calculated. A temperature of 1100°C is adopted for the magma, based in part upon the studies of Barton and Hamilton (1978) on Leucite Hills lavas. At 1100°C, 1 bar, and oxygen fugacities of the FMQ buffer, the Fe–Mg interdiffusion coefficient along c for Fo_{85} olivine can be approximated as 3×10^{-11} cm²/sec from the algorithms of Buening and Buseck (1973); at 1100°C, they show that the coefficients for magnesian olivine in the a and b directions are about ¼ that in the c direction. Their data also document a decrease in diffusivity with decreasing oxygen fugacity as well as with decreasing temperature, and Misener (1974) showed a decrease with increasing pressure. In view of the uncertainties in temperature, oxygen fugacity, pressure, and exact crystallographic direction, a value of 10^{-11} cm²/sec was adopted here for interpretation of olivine profiles. For comparison with the observed profiles, Fe–Mg gradients were calculated with this D for a model of a "semi-infinite" medium, initially at a constant composition, starting at zero time, as described in standard references (e.g., Shewmon, 1963). The model was chosen for diffusion between the olivine and a grain-boundary melt partly because diffusion in a melt is much faster than in olivine; the model presumes that the melt composition at the olivine interface does not change with time. Though the model clearly is an idealization and likely to be wrong in detail, more sophisticated models are not justified by the necessary assumptions and by the data. A profile for normalized Fe–Mg variations in the b direction in an olivine crystal is compared to curves calculated for an elapsed time of 2.25×10^5 seconds (63 hours) in Figure 5. Profiles measured in other olivine grains were best fit with the model by times in the range 1.7×10^5 to 2.8×10^5 seconds.

The time of 63 hours may approximate residence time in the magma, and it is useful for estimates of diffusivities in the spinels. No data are available for the diffusivity of Ca in olivine, and we do not attempt to estimate a value here, both because counting statistics are poor and because the expression of Hervig (1979) indicates that a change of 20 kbar at 1100°C changes the Ca content of olivine in equilibrium with orthopyroxene (and likely with a melt) by more than a factor of two. In contrast, the Fe–Mg partition between olivine and melts is relatively insensitive to pressure (Longhi et al., 1978). Visual comparison of the gradients in Figure 3A, however, suggests that the effective binary diffusion coefficient of Ca is substantially lower than the interdiffusion coefficient for Fe–Mg.

Gradients at pleonaste-magnetite contacts

Compositional data for three element groups were measured in traverses in four composite spinel grains; six elements were measured across two boundaries, and the results in one case are shown in Figure 4. All essential characteristics of Figure 4, including the unusual behavior of Cr, were observed for at least one other contact.

The gradients which formed in the same time interval in both spinels and in olivine provide opportunities to compare diffusivities in these phases, but simple, exact comparisons are impossible. While only Fe and Mg are important diffusing species in olivine, diffusion of Al, Fe, Mg, and Cr must be considered in treating diffusion in the spinel pairs. Multicomponent diffusion has been discussed recently by Lasaga (1979) and Loomis (1978): in the general case the flux of any diffusing species equals the sum of products of diffusion coefficients and chemical potential gradients for all but one of the other diffusing species (one is dependent, by stoichiometry). During such an irreversible process, diffusion of a species up its concentration gradient or even up its chemical potential gradient will be a common feature (Cooper, 1974). The increase in Cr at the two-spinel contact is best explained by such a transient, kinetic effect, since two-spinel tielines on a Al–Cr–Fe^{3+} diagram are approximately parallel for a range of YCr and Mg/(Mg + Fe^{2+}) values (Fig. 3 of Steele et al., 1977). If diffusion coefficients were independent of composition, then the Cr profile would be symmetric about the original interface; the asymmetry suggests that the coefficients are strongly concentration dependent, further complicating analysis of the gradients. For "semi-infinite diffusion couples" like those examined
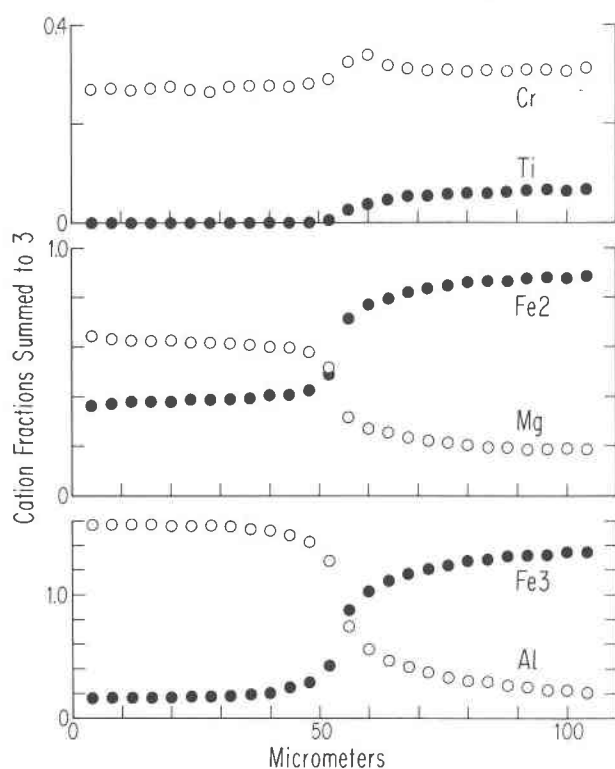
Fig. 4. Cation fractions from a traverse with 4 μm steps across the boundary between pleonaste and magnetite in the composite grain shown in Fig. 1a. Note the changes in scale, and the increase in Cr near the contact. Cation fractions were determined from the sum of atomic proportions of Fe, Cr, Al, Ti, and Mg normalized to 3; ferrous and ferric iron were calculated assuming 4 oxygens. Data are from two traverses—one for Fe, Cr, Al and the other for Fe, Ti, Mg—measured along nearly the same path, and hence a mismatch of several micrometers is possible in comparing the Cr–Al values with those for Ti–Mg.

here, Cooper (1968) has justified the concept of "effective binary diffusion coefficients" (EBDC's), which are valid for particular composition couples. The diffusivities in spinel discussed below can be considered as EBDC's averaged over compositional ranges and temperature.

The spinel data should fit the simple model of a pair of "semi-infinite" homogeneous solids joined on a planar contact at zero time and partly homogenized, since the temperature of the minette magma must have been well above the spinel miscibility gap. In the simplest case the model can be described by a solution of the general form $Cn = 0.5 (1\pm erf(x/\sqrt{4Dt}))$, where Cn is the normalized concentration, D a constant diffusivity, t the time, and x the distance from the contact. Exactly the same equation fits diffusion gradients in an initially homogeneous, "semi-infinite" solid with its planar contact held at a differ-

ent, constant composition—the model assumed for olivine. Only the value of the normalized concentration, Cn, differs, being 1 for spinel at the planar interface at zero time and 0.5 for olivine at the planar interface for all times after 0.

Since the models are fit by the same equation, normalized Al_2O_3 and MgO gradients across a two-spinel contact and FeO and MgO gradients in an olivine crystal are plotted together in Figure 5 for ready comparison. The MgO data for olivine fit this form of solution very well; the slight misfit for iron could reflect secondary fluorescence of iron in adjacent magnetite. In contrast, the spinel data deviate markedly from the solutions plotted in Figure 5, probably because the EBDC's are functions of composition, and the compositional range for spinel before normalization is much greater than that for olivine. The comparison indicates that average EBDC's for Al and Mg in both spinels are distinctly less than the average interdiffusion coefficient for Fe and Mg in olivine; assuming an average value of 10^{-11} cm^2/sec for olivine, EBDC's for Al appear near 10^{-11} and 10^{-12} in magnetite and pleonaste, respectively. EBDC's for Mg lie in the same range but with a different compositional dependence.

Discussion

The EBDC's inferred for Al and Mg in the spinel phases are similar to measured diffusion coefficients for simpler systems. The Fe–Ti interdiffusion coefficient in magnetite at 3% Ti and 1100°C is 2.5×10^{-11} cm^2/sec (Freer and Hauptman, 1978). The self-diffusion coefficient for Mg in $MgAl_2O_4$ is about 4×10^{-12} cm^2/sec at 1100°C (Lindner and Akerstrom, 1958). Birchenall (1968) noted that the general mobility of cations in magnetite-rich spinels is clearly greater than in aluminum-rich ones, as observed here for Al. Calculation of the complete matrices of diffusion coefficients for natural spinels requires a knowledge of tracer diffusion coefficients for all species plus activity-composition relations (Lasaga, 1979); furthermore, diffusivities in iron-bearing spinels may depend on oxygen fugacity in a complex fashion (Dieckmann and Schmalzried, 1977). Since few of the experimental data directly applicable to natural spinels are available, the order-of-magnitude EBDC's inferred here are useful guides to cation mobilities in them.

The diffusivities can be used to estimate homogenization and exsolution times. If the composite spinel grains are modelled as rectangular parallelopipeds of length 2h, equations of Crank (1956) can be used to
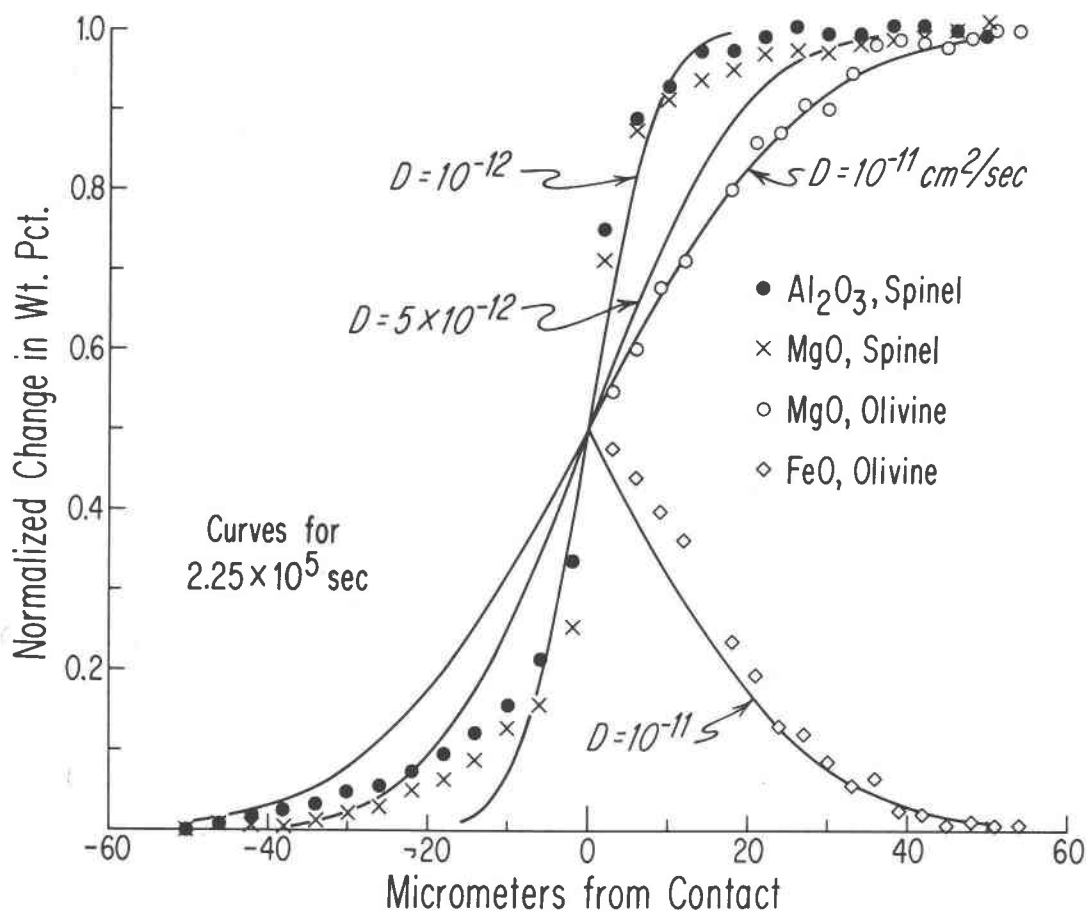
Fig. 5. Normalized, measured diffusion gradients and calculated profiles both for a pleonaste–magnetite couple in the interior of a composite spinel grain and for an olivine crystal in contact with a presumed boundary melt adjacent to magnetite. The same data were used in Figs. 3A and 4; here, weight percent changes for MgO and Al_2O_3 in the spinel couple were normalized to 1, and changes for MgO and FeO in olivine were normalized to 0.5. Though different diffusion models are used for the spinel couple and for the olivine-boundary melt (see text), with the normalization procedure the same calculated profiles are appropriate for both models. The calculated profiles assume constant diffusivities (D's) and a time of 225,000 seconds (63 hours).

show nearly complete homogenization in a time of h^2/D and substantial homogenization in $h^2/4D$ (constant D, binary interdiffusion). Using the latter equation, a one-mm-long, composite grain would show substantial homogenization or granule exsolution in about 20 years ($D = 10^{-12}$) or 2 years (10^{-11}). Birchenall (1968) estimated that activation energies for cation mobility are typically near 280 kj for ferrite spinels and 380 kj for aluminate spinels, while Freer and Hauptman (1978) found a value near 215 kj for Fe–Ti interdiffusion in titanium-poor magnetite. These values are significantly larger than that of 150 kj averaged for the data of Buening and Buseck (1973) for magnesian olivine from 1000–1125°C at constant oxygen fugacity; the olivine value would be greater along a buffer curve, but still less than the values estimated for spinels by Birchenall. Assuming a value of

10^{-11} cm²/sec at 1100°C and an activation energy of 350 kj for spinel, these approximate D's (cm²/sec) and times for substantial homogenization ($h^2/4D$, h = .5 mm) can be calculated: 1300°C—5 × 10^{-10}, 14 days; 1200°C—8 × 10^{-11}, 90 days; 1100°C—10^{-11}, 2 years; 800°C—2 × 10^{-15}, 10^4 years; 700°C—3 × 10^{-17}, 7 × 10^5 years. The annealing experiments by Roeder et al. (1979) on olivine–chromite rocks showed no equilibration after heating at 1100°C, partial re-equilibration at 1200°C for 14 days, and extensive re-equilibration at 1300°C for 50 hours. Their results suggest that diffusivities and/or activation energies for chromites near the FMQ buffer are somewhat greater than the values used above, but the grain sizes of their samples were not specified, and precise comparisons cannot be made. Temperatures near 500°C calculated by Roeder et al. (1979) for oli-

vine-chromite pairs from several large layered intrusions also suggest higher diffusivities at low temperatures, if their geothermometer is reliable for chromite-olivine in this range. Regardless, it is clear that long equilibration times at 700°C are required to produce homogeneous spinel pairs like those in the inclusion studied here; mantle cooling (Stage I) could provide such time, while many crustal situations would not (Engi, 1978). Extensive chromite-silicate exchange in layered, crustal intrusions like that discussed by Irvine (1967) must also be the result of very slow cooling, unless cation mobility is enhanced by much higher oxygen fugacities (as it is in magnetite, Dieckmann and Schmalzried, 1977) or by lattice disruption and recrystallization during oxidation reactions. Such reactions may explain the relatively coarse oxide intergrowths produced by oxidation-exsolution during cooling in many rocks (*e.g.*, Haggerty, 1976).

The apparent stability of gradients in spinel and olivine during cooling in minette at the surface is probably due to a high rate of heat loss. Fe–Mg profiles in olivine, as calculated by Taylor *et al.* (1977), show little change below 1000°C at cooling rates exceeding 5°C per day. Since cation mobility is less in the spinels and activation energies are likely to be greater, spinel gradients might be "frozen in" at higher temperatures and/or slower rates of cooling. Gradients in olivine and spinel at mutual contacts are not uncommon (Clark, 1978), and their analysis by methods of Lasaga *et al.* (1977) and Lasaga (1979) may provide a method to estimate cooling rates. The Cr variations observed here (Fig. 4) indicate the complexities which diffusion may produce in the multicomponent gradients.

Regional considerations

Both mafic and felsic minettes occur in the Navajo province; the varieties are generally thought to be related by mantle processes, but some evidence suggests interaction with the crust (Ehrenberg, 1977; Roden and Smith, 1979; Roden, ms). Roden (1977) determined that some magma of each variety rose through the crust in a short time, 10 hours or less; his calculations were based upon sizes and densities of peridotite inclusions, estimated magma densities and viscosities, and the assumption of Newtonian behavior. If the magmas had yield strengths (*e.g.,* Sparks *et al.* 1977), then the calculations could grossly underestimate crustal residence times. The times near 60 hours calculated here for generation of gradients in

olivine after the peridotite was sampled by the minette magma are broadly consistent with the shorter ascent times calculated assuming Newtonian viscosity, since the diffusion time must reflect both any preheating and the crystallization time of the minette lava on the surface. Uncertainties in the temperature history, oxygen fugacity, and history of the grain boundary melts add additional uncertainty to the calculated diffusion time. Nonetheless, the fact that two independent calculations yield short ascent times is evidence for a limited crustal residence period for the minette magma. The limited time supports hypotheses that the dominant geochemical characteristics of the minettes formed in the mantle, not by extensive magma-crust interaction.

The pipes of serpentinized ultramafic microbreccia (Plateau "kimberlite") within 8 km of the xenolith locality contain many inclusions of partly hydrated and carbonated peridotite. Smith and Levy (1976) and Smith (1979) inferred that the hydrous phases in the inclusions formed at temperatures below 700°C in the uppermost mantle. Ehrenberg and Griffin (1979) suggest that the hydration of spinel lherzolites may have occurred within the crust as ultramafic diapirs rose upwards. The temperature near or below 700°C estimated here for mantle equilibration of the peridotite inclusion is evidence that low-temperature histories also characterize some mantle sampled by minette, so temperatures suitable for hydration likely did occur within the uppermost mantle at the time of minette-"kimberlite" eruption.

Acknowledgments

References

Albee, A. L. and Ray, L. (1970) Correction factors for electron probe micro-analysis of silicates, oxides, carbonates, phosphates, and sulfates. Analytical Chemistry, 42, 1408–1414.

Allen, J. E. and Balk, R. (1954) Mineral resources of Fort Defiance and Tohatchi quadrangles, Arizona and New Mexico. New Mexico Bureau of Mines and Mineral Resources Bulletin, 35, 140 p.

Barton, M. and Hamilton, D. L. (1978) Water-saturated melting relations to 5 kilobars of three Leucite Hills lavas. Contributions to Mineralogy and Petrology, 66, 41–49.

Bence, A. E. and Albee, A. L. (1968) Empirical correction factors for the electron microanalysis of silicates and oxides. Journal of Geology, 26, 382–403.

Berg, J. H. (1976) Metamorphosed mafic and ultramafic rocks in

the contact aureoles of the Nain complex, Labrador, and the miscibility gap between spinel and magnetite in natural Cr–Al–Fe3–Ti spinels. Geological Society of America Abstracts with Programs, 8, 773–774.

Birchenall, C. E. (1968) Diffusion in oxides: assessment of existing data and experimental problems. In J. B. Wachtman and A. D. Franklin, Eds., Mass Transport In Oxides, National Bureau of Standards Special Publications, 296, 119–127.

Buening, D. K. and Buseck, P. R. (1973) Fe–Mg lattice diffusion in olivine. Journal of Geophysical Research, 78, 6852–6862.

Clark, A. T. (1978) Oxide minerals in the Turnagain ultramafic complex, northwestern British Columbia. Canadian Journal of Earth Sciences, 15, 1893–1903.

Cooper, A. R. (1968) The use and limitations of the concept of an effective binary diffusion coefficient for multi-component diffusion. In J. B. Wachtman and A. D. Franklin, Eds., Mass Transport In Oxides, National Bureau of Standards Special Publications, 296, 79–84.

Cooper, A. R. (1974) Vector space treatment of multicomponent diffusion. In A. W. Hofmann et al., Eds., Chemical Transport and Kinetics, Carnegie Institution of Washington Publication, 634, 15–30.

Crank, J. (1956) The Mathematics of Diffusion. Oxford University Press, London.

Danckwerth, A. and Newton, R. C. (1978) Experimental determination of the spinel peridotite to garnet peridotite reaction in the system MgO–Al$_2$O$_3$–SiO$_2$ in the range 900°–1100°C and Al$_2$O$_3$ isopleths of enstatite in the spinel field. Contributions to Mineralogy and Petrology, 66, 189–201.

Dieckmann, R. and Schmalzried, H. (1977) Defects and cation diffusion in magnetite. Berichte der Bunsen-Gesellschaft, 81, 344–347.

Ehrenberg, S. N. (1977) The Washington Pass volcanic center: evolution and eruption of minette magmas of the Navajo volcanic field. Extended Abstracts of the Second International Kimberlite Conference, American Geophysical Union.

Ehrenberg, S. N. (1979) Garnetiferous ultramafic inclusions in minette from the Navajo volcanic field. In F. R. Boyd and H. O. A. Meyer, Eds., The Mantle Sample: Inclusions in Kimberlites and Other Volcanics, p. 330–344. American Geophysical Union.

Ehrenberg, S. N. and Griffin, W. L. (1979) Garnet granulite and associated xenoliths in minette and serpentinite diatremes of the Colorado Plateau. Geology, 7, 483–487.

Engi, M. (1978) Olivine-spinel geothermometry: an experimental study of the magnesium-iron exchange. (abstr.) EOS, 59, 401.

Evans, B. W. and Frost, B. R. (1975) Chrome-spinel in progressive metamorphism—a preliminary analysis. Geochimica et Cosmochimica Acta, 39, 959–972.

Fabries, J. (1979) Spinel-olivine geothermometry in peridotites from ultramafic complexes. Contributions to Mineralogy and Petrology, 69, 329–336.

Finnerty, A. A. and Boyd, F. R. (1979) Comparison of thermobarometers for garnet peridotites. (abstr.) Geological Society of America Abstracts with Programs, 11, 426.

Freer, R. and Hauptman, Z. (1978) An experimental study of magnetite-titanomagnetite interdiffusion. Physics of Earth and Planetary Interiors, 16, 223–231.

Frey, F. A. and Prinz, M. (1978) Ultramafic inclusions from San Carlos, Arizona: petrologic and geochemical data bearing on their petrogenesis. Earth and Planetary Science Letters, 38, 129–176.

Fujii, T. (1978) Fe–Mg partitioning between olivine and spinel. Carnegie Institution of Washington Year Book, 76, 563–569.

Haggerty, S. E. (1976) Opaque mineral oxides in terrestrial igneous rocks. In D. Rumble, Ed., Oxide Minerals, Mineralogical Society of America Short Course Notes, 3, 101–277.

Harte, B. (1977) Rock nomenclature with particular relation to deformation and recrystallization textures in olivine-bearing xenoliths. Journal of Geology, 85, 279–288.

Hervig, R. L. (1979) Ca–Mg exchange between olivine and orthopyroxene: a geobarometer for garnet and spinel lherzolites. (abstr.) Geological Society of America Abstracts with Programs, 11, 443.

Irvine, T. N. (1967) Chromian spinel as a petrogenetic indicator—Part 2. Petrologic applications. Canadian Journal of Earth Sciences, 4, 71–103.

Lasaga, A. C. (1979) Multicomponent exchange and diffusion in silicates. Geochimica et Cosmochimica Acta, 43, 455–469.

Lasaga, A. C., Richardson, S. M. and Holland, H. D. (1977) The mathematics of cation diffusion and exchange between silicate minerals during retrograde metamorphism. In S. K. Saxena and S. Bhattacharji, Eds., Energetics of Geological Processes, p. 353–388, Springer-Verlag, New York.

Lindner, R. and Akerstrom, A. (1958) Diffusion von Ni–63 in nickelspinellen: Zeitschrift fur Physikalische Chemie Neue Folge, 18, 303–307.

Loomis, T. P. (1978) Multicomponent diffusion in garnet: I. Formulation of isothermal models. American Journal of Science, 278, 1099–1118.

Longhi, J., Walker, D. and Hays, J. F. (1978) The distribution of Fe and Mg between olivine and lunar basaltic liquids. Geochimica et Cosmochimica Acta, 42, 1545–1558.

Misener, J. (1974) Cationic diffusion in olivine to 1400°C and 35 kb. In A. W. Hofmann et al., Eds., Geochemical Transport and Kinetics. Carnegie Institution of Washington Publication, 634, 117–130.

Muir, J. E. and Naldrett, A. J. (1973) A natural occurrence of two-phase chromium-bearing spinels. Canadian Mineralogist, 11, 930–939.

Roden, M. F. (1977) Field geology and petrology of the minette diatreme at Buell Park, Apache Country, Arizona. M. A. Thesis, University of Texas, Austin.

Roden, M. F., Smith, D. and McDowell, F. W. (1979) Age and extent of potassic volcanism on the Colorado Plateau. Earth and Planetary Science Letters, 43, 279–284.

Roden, M. F. and Smith, D. (1979) Field geology, chemistry and petrology of Buell Park minette diatreme, Apache County, Arizona. In F. R. Boyd and H. O. A. Meyer, Eds., Kimberlites, Diatremes, and Diamonds: Their Geology, Petrology, and Geochemistry: Proceedings of the Second International Kimberlite Conference, 1, 364–381.

Roeder, P. L., Campbell, I. H. and Jamieson, H. E. (1979) A re-evaluation of the olivine-spinel geothermometer. Contributions to Mineralogy and Petrology, 68, 325–334.

Shewmon, P. G. (1963) Diffusion in Solids. McGraw-Hill, New York.

Silver, L. T. (1963) The use of cogenetic uranium-lead isotope systems in zircons in geochronology. In Radioactive Dating, Proceedings Series of the International Atomic Energy Agency (Vienna), 279–287.

Smith, D. (1979) Hydrous minerals and carbonates in peridotite inclusions from the Green Knobs and Buell Park kimberlitic diatremes on the Colorado Plateau. In F. R. Boyd and H. O. A.

Meyer, Eds., The Mantle Sample: Inclusions in Kimberlites and Other Volcanics: Proceedings of the Second International Kimberlite Conference, 2, 345–356.

Smith, D. and Levy, S. (1976) Petrology of the Green Knobs diatreme and implications for the upper mantle below the Colorado Plateau. Earth and Planetary Science Letters, 29, 107–125.

Sparks, R. S. J., Pinkerton, H. and MacDonald, R. (1977) The transport of xenoliths in magmas. Earth and Planetary Science Letters, 35, 234–238.

Springer, R. K. (1974) Contact metamorphosed ultramafic rocks in the western Sierra Nevada Foothills, California. Journal of Petrology, 15, 160–195.

Steele, I. M., Bishop, F. C., Smith, J. V. and Windley, B. F. (1977) The Fiskenaesset complex, West Greeenland, Part III. Gronlands Geologiske Undersogelse Bulletin, 124, 38 p.

Taylor, L. A., Onorato, P. I. K. and Uhlmann, D. R. (1977) Cooling rate estimations based on kinetic modelling of Fe–Mg diffusion in olivine. Proceedings of the 8th Lunar Science Conference, 1581–1592.

Turnock, A. C. and Eugster, H. P. (1962) Fe–Al oxides: phase relationships below 1000°C. Journal of Petrology, 3, 533–565.

Wells, P. R. A. (1977) Pyroxene thermometry in simple and complex systems. Contributions to Mineralogy and Petrology, 62, 129–139.

White, R. W. (1966) Ultramafic inclusions in basaltic rocks from Hawaii. Contributions to Mineralogy and Petrology, 12, 245–314.